DISCRETE ELEMENT MODELLING TO PREDICT FAILURE STRENGTH OF UNREINFORCED MASONRY WALLS

F. Gálvez[1a]; K. Ip[1b]; J. Vaculik[2a]; M.C. Griffith[2b]; L. Sorrentino[3]; D. Dizhur[4a]; J.M. Ingham[4b]

1. a) Corresponding Author, PhD Candidate. b) PhD Candidate. Department of Civil & Environmental Engineering, The University of Auckland, Private Bag 92019, Auckland 1010, New Zealand. Email: fglv390@aucklanduni.ac.nz, cip314@aucklanduni.ac.nz

2. a) Postdoctoral Research Fellow. b) Professor. School of Civil, Environmental and Mining Engineering, The University of Adelaide, SA 5005, Australia. Email: jaroslav.vaculik@adelaide.edu.au, michael.griffith@adelaide.edu.au

3. Assisstant Professor, Sapienza Università di Roma, Dipartimento di Ingegneria Strutturale e Geotecnica, via Antonio Gramsci 53, 00197 Roma, Italy. Email: luigi.sorrentino@uniroma1.it

4. a) Lecturer. b) Professor. Department of Civil & Environmental Engineering, The University of Auckland, Private Bag 92019, Auckland 1010, New Zealand. Email: ddiz001@aucklanduni.ac.nz, j.ingham@auckland.ac.nz

Abstract

Similar unreinforced masonry (URM) buildings are found in Australia and New Zealand due to the two countries' shared history of European settlement. It is known that there is a large inventory of URM buildings in both countries and that these buildings are potentially earthquake prone. Therefore, an understanding of their behaviour when subjected to earthquake loading is needed. The Discrete Element Method (DEM) is an advanced modelling technique that can accurately predict and simulate collapse mechanisms in a realistic way. In the reported study the DEM was applied using a micro-modelling approach to simulate walls tested in the laboratory. Solid rigid elements were used to represent the distinct brick units and an inelastic law was assigned to the contact surfaces to simulate the mortar between the bricks.

In previous work two groups of walls were tested. First, full-scale walls with different configurations were subjected to quasi-static face loading imposed by a system of airbags. Secondly, five reduced scale walls were built for shaking-table testing. Non-linear static (pushover) analysis was conducted to simulate the first group of walls of the experimental campaign. In addition to the wall simulations, simple brick and mortar numerical models were generated and analysed for calibration purposes.

Keywords: DEM, URM, Walls, Failure Mechanisms, Out-of-plane

1. INTRODUCTION

Despite the relatively simple methods used to construct unreinforced masonry (URM) structures, their complex internal mechanical behaviour complicates the simulation of URM buildings or URM structural components. However, several assumptions and shortcuts can be taken to obtain fast and reasonably accurate results to simulate masonry structures. Lourenço (2002) described different approaches or strategies for numerical modelling of URM that can be classified as either macro or micro modelling.

Post-earthquake observations have shown the importance of out-of-plane failure mechanisms of the walls in URM buildings (Leite et al., 2013). When a wall is subjected to out-of-plane loads such as those arising from wind or earthquake, a flexural deformation (bending) is experienced, which readily causes cracks due to the low tensile strength of URM. Although URM walls are more vulnerable in their out-of-plane direction, in-plane response has been more widely studied. Several authors have studied out-of-plane behaviour of dry-joint or mortared masonry walls using the Discrete Element Method (DEM) (Baraldi & Cecchi, 2017; Çaktı et al., 2016; Giamundo et al., 2014).

A series of walls that varied in their dimensions and geometry (see Figure 1) was subjected to out-of-plane loading by Griffith and Vaculik (2007). Capacity curves and collapse mechanisms were registered and analytical formulae were developed for the assessment of URM walls. The code 3DEC formulated by Itasca (2013) was used in the reported study to simulate the outcome of the experimental data.

2. MODELLING APPROACH

As stated in Lawrence and Marshal (1996), two-way spanning walls undergo biaxial bending by provoking a complex failure mechanism which includes horizontal and vertical stresses at the mortar interfaces, generating a combination of horizontal, vertical, and diagonal crack patterns. The observed crack patterns in the Griffith and Vaculik (2007) experiments agreed with the notion that deformation behaviour is dependent on the number and type of boundary conditions, and were mainly localized within the mortar joints. The performed tests in units and mortar showed unit properties of E: 52,700 MPa and ft: 3.55 MPa, while mortar presented E: 442 MPa. Similar mortar was tested by Van der Pluijm (1997) performing ft: 0.22-0.32MPa.

Based on the above observation, brick blocks were modelled using rigid polyhedral elements allowing no deformation, and consequently cracks did not form through the bricks. Each block interacted with its neighbours through a non-linear contact joint that represented the mortar interface. The lintel above the opening was also modelled using rigid bricks, but the contact joints were modelled with a higher stiffness and strength. Each contact joint was governed by a Mohr-Coulomb model characterised by five normal and shear parameters: normal stiffness (j_{kn}); shear stiffness (j_{ks}); friction angle ($^{\circ}$); cohesion (c); and tensile strength (f_t). Once the onset of failure was identified at the sub-contacts into which the joint contact was divided, in either tension or shear, the tensile strength and cohesion were taken as zero. This computationally economical approach has been widely used by other authors (Bui & Limam, 2013; Çaktı et al., 2016) to model unreinforced masonry structures. No crushing of bricks was observed during the experimental campaign, and this observation confirms the assumption that a linear compression constitutive relation was a reasonable modelling strategy.

In addition to the wall tests, Griffith and Vaculik (2007) tested the material properties of different batches of bricks and mortar corresponding to each wall. Although the same volumetric ratio of components was used to make the mortar and the same type of bricks were used in each test, different values of modulus of elasticity, tensile strength, and compressive strength were obtained. The reason for such differences could be associated with a range of different sources, such as variations in workmanship and handling, temperature and humidity alteration, or slight differences in the volumetric ratios. Therefore, the tensile strength and elasticity parameters were calibrated by trial and error to match the experiments.

Panel dimensions [mm] and support arrangement	Wall	σ_{vo} [MPa]
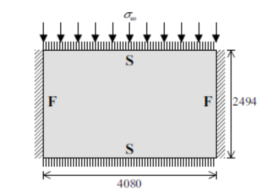	s1	0.10
	s2	0
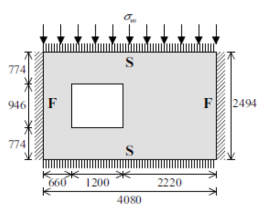	s3	0.10
	s4	0.05
	s5	0
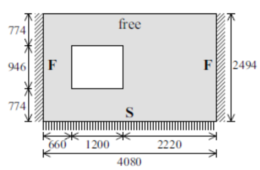	s6	–
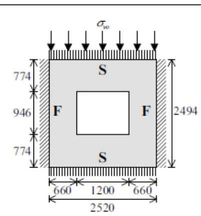	s7	0.10
	s8	0

Note: F = Fixed support, S = Simple support

(a) Test wall configurations (Griffith & Vaculik, 2007)

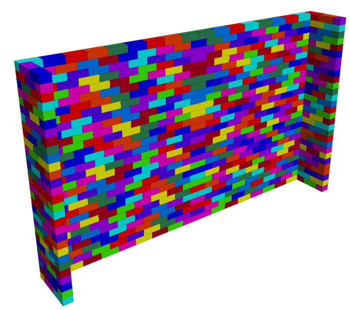

(b) Geometry of numerical model

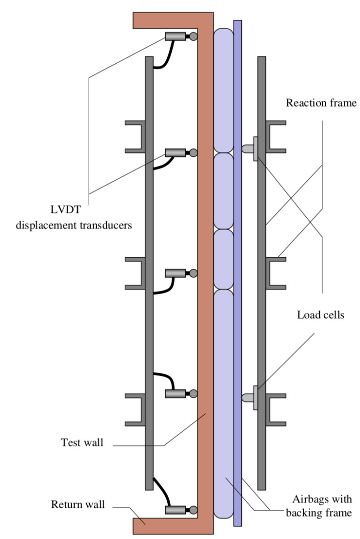

(c) Plan view of ultimate strength test (Griffith & Vaculik, 2007)

Figure 1: Test and simulation configuration

Different approaches were considered to simulate the boundary conditions (see Figure 2). First, the bricks in the boundary of the wall were considered as fixed. Next, the boundary constraints were modelled in the same manner as they were built in the laboratory. And finally, the option that best represented the experiments and showed a better response match was modelling by using a masonry frame along the boundary (Figure 2c) with a high joint stiffness sufficient to be considered as rigid. This last option illustrated the need for a certain amount of rotational degree of freedom in the boundary conditions.

Reacting forces in the perpendicular direction of the wall were computed from the lowest row of fixed blocks to calculate the reacting pressure, while the displacement was computed by considering the brick in the location closest to the position specified in Griffith and Vaculik (2007). The distributed pressure that was applied in the experiments by deploying inflating airbags was simulated by subjecting each brick to equal increasing pressure. Boundary bricks were not loaded to account for boundary effects at the edge of the bags. The collapse mechanisms were studied by plotting the normal displacement of the joints (Figure 3).

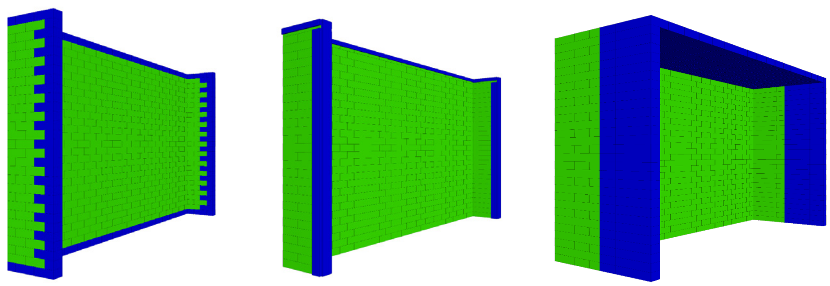

(a) (b) (c)

Figure 2: Boundary conditions studied

3DEC uses adaptive global damping to adjust the damping constant automatically. Viscous damping forces are used, but the viscosity constant is continuously adjusted in such a way that the power absorbed by damping is a constant proportion of the rate of change of kinetic energy in the system (Itasca, 2013). An overdamped system was considered sufficient to simulate the quasi-static pushover experiments.

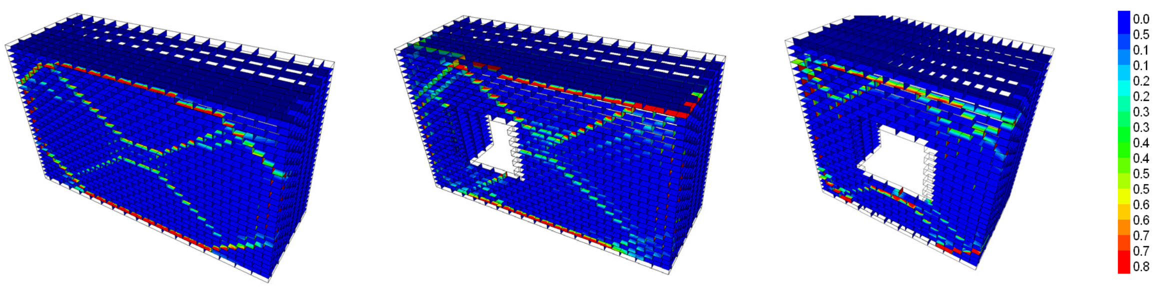

Figure 3: Crack opening examples for the three wall configurations (crack widths in mm units)

3. RESULTS

3.1. MATERIAL CALIBRATION

Van der Pluijm (1992, 1993) conducted tensile and shear tests measuring the displacement of solid clay and calcium silicate bricks with a mortar layer between the brick units. The tensile behaviour was found to exhibit exponential results that describe a Mode I fracture energy. Different levels of compressive stress were constantly applied normal to the mortar interface during the shear tests. After the maximum strength was reached an exponential softening that led to a frictional residual interaction was observed. Frictional interactions increased in proportion to the level of confinement applied, as seen in Figure 4b. The area defined underneath the stress-displacement curve in the absence of a normal confining load is defined as the Mode II fracture energy. For an understanding of the constitutive law adopted and the approximation of the behaviour in the tensile and shear range, the tests were modelled and compared with the results of the simulation (Figure 4).

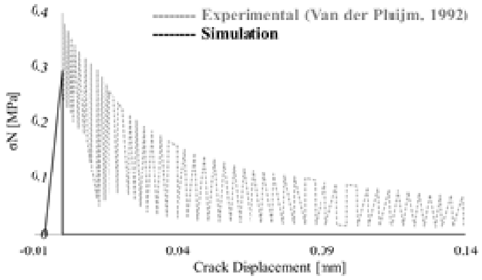

(a) Tensile behaviour of brick-mortar interaction

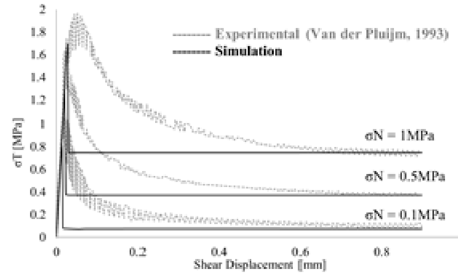

(b) Shear behaviour of brick-mortar interaction

Figure 4: Coulomb slip model vs experimental results (Van der Pluijm, 1992, 1993), with j_{kn}=77e3 MPa/m; j_{ks}=63e3 MPa/m; fric=36.87°; f_t = 0.3 MPa; c=0.95 MPa.

3.2. FULL SCALE WALLS

Eight full scale URM walls were built using Australian clay bricks with dimensions 230 × 110 × 76 mm^3 (length × thickness × height), perforated with two rows of five holes. The bricks were assembled with mortar layers of 10 mm in thickness using the volumetric ratio 1:2:9 (cement:lime:sand). The density of the masonry walls were 1900 kg/m^3. Within the variety of combinations of tested walls, six walls contained an opening and four walls were subjected to vertical pre-compression (Figure 1a). These walls were subjected to quasi-static face loading imposed by a system of airbags connected to a pump controlled by software, as seen in Figure 1c. The test consisted of deforming the walls to their ultimate strength, followed by gradual unloading. The outcome of the simulations are shown in Figure 6-Figure 12, where cracks in the outer face of the walls are drawn in red, whereas green is used for the cracks in the inner face.

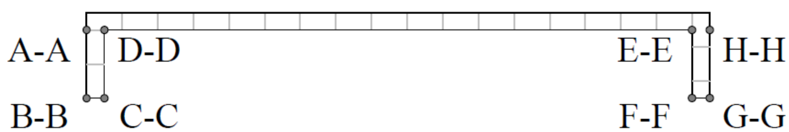

Figure 5: Wall Reference Geometry

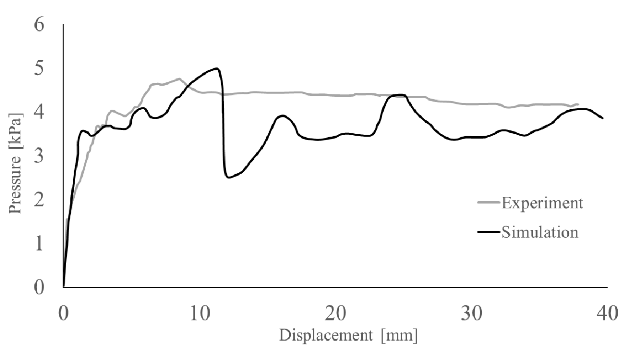

(a) Pressure-displacement diagram

Material properties: fric=30°; c=0.37 MPa; f_t=0.35 MPa

Horizontal joints

j_{kn}=37e3 MPa/m; j_{ks}=31.4e3 MPa/m

Vertical joints

j_{kn}=13.3e3 MPa/m; j_{ks}=11.3e3 MPa/m

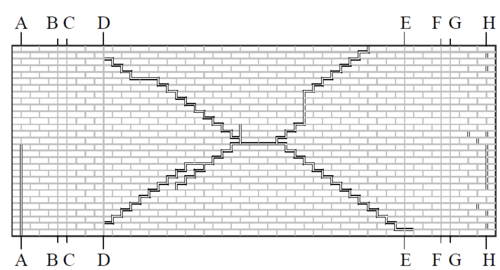

(b) Experimental crack pattern

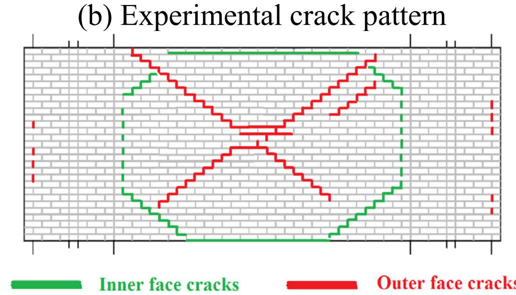

(c) Simulation crack pattern

Figure 6: Wall S1

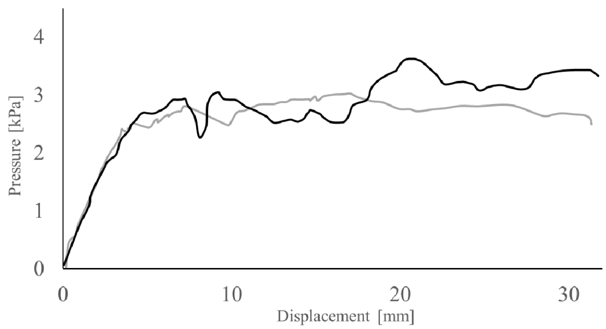

(a) Pressure-displacement diagram

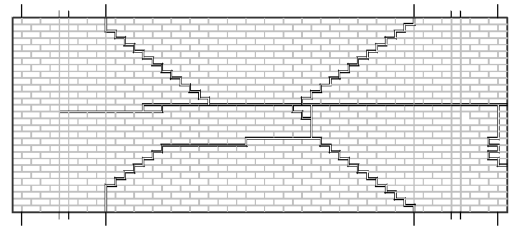

(b) Experimental crack pattern

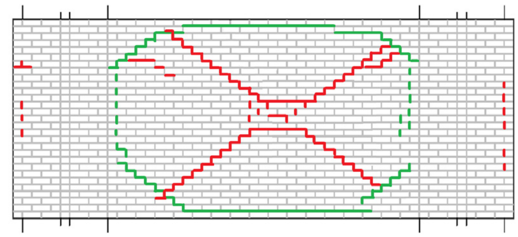

(c) Simulation crack pattern

Material properties: fric=30°; c=0.27 MPa; f_t=0.25 MPa

Horizontal joints

j_{kn}=6.6e3 MPa/m; j_{ks}=5.8e3 MPa/m

Vertical joints

j_{kn}=2.4e3 MPa/m; j_{ks}=2.1e3 MPa/m

Figure 7: Wall S2

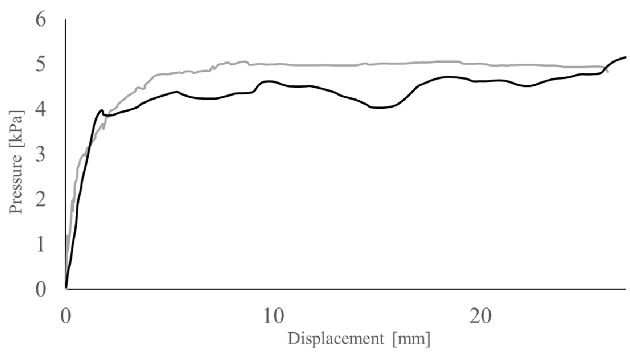

(a) Pressure-displacement diagram

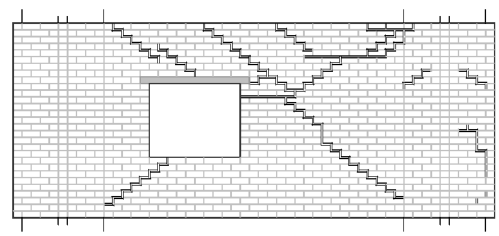

(b) Experimental crack pattern

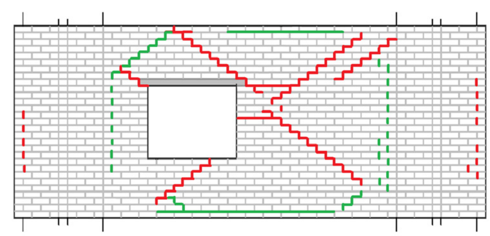

(c) Simulation crack pattern

Material properties: fric=30°; c=0.25 MPa; f_t=0.23 MPa

Horizontal joints

j_{kn}=28.5e3 MPa/m; j_{ks}=24.1e3 MPa/m

Vertical joints

j_{kn}=10e3 MPa/m; j_{ks}=8.6e3 MPa/m

Figure 8: Wall S3

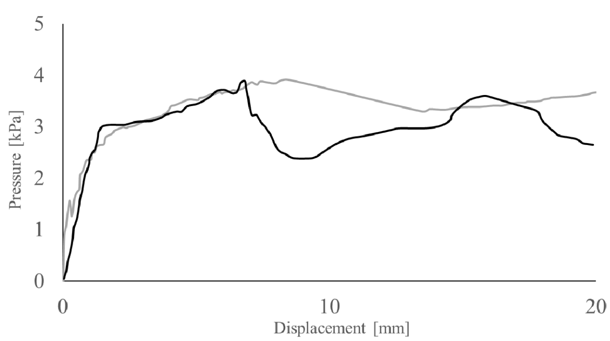

(a) Pressure-displacement diagram

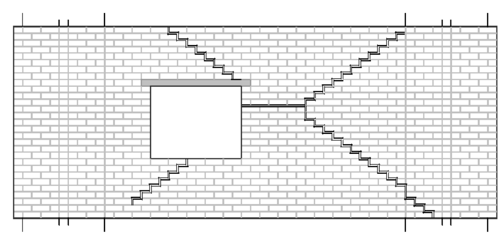

(b) Experimental crack pattern

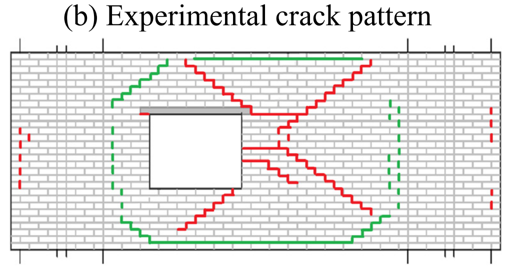

(c) Simulation crack pattern

Material properties: fric=30°; c=0.21 MPa; f_t=0.19 MPa

Horizontal joints

j_{kn}=19.8e3 MPa/m; j_{ks}=16.8e3 MPa/m

Vertical joints

j_{kn}=7.2e3 MPa/m; j_{ks}=6e3 MPa/m

Figure 9: Wall S4

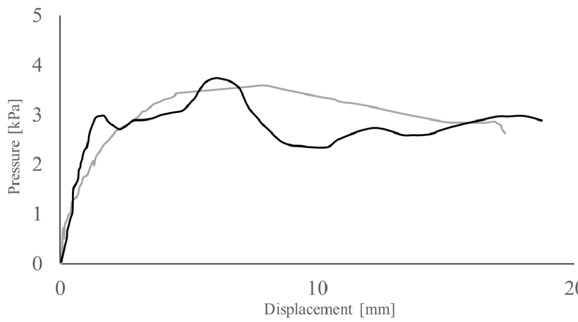

(a) Pressure-displacement diagram

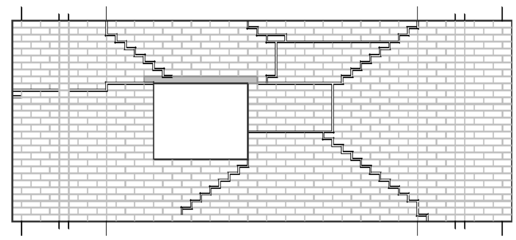

(b) Experimental crack pattern

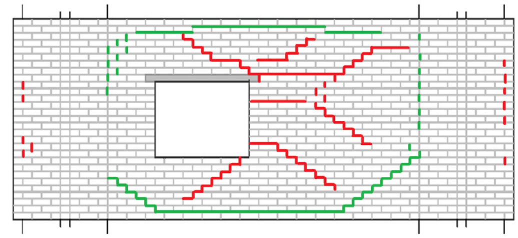

(c) Simulation crack pattern

Material properties: fric=30°; c=0.21 MPa; f_t=0.19 MPa

Horizontal joints

j_{kn}=19.8e3 MPa/m; j_{ks}=16.8e3 MPa/m

Vertical joints

j_{kn}=7.2e3 MPa/m; j_{ks}=6e3 MPa/m

Figure 10: Wall S5

(a)

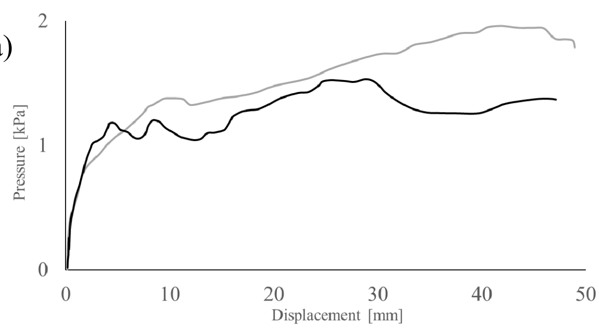

(a) Pressure-displacement diagram

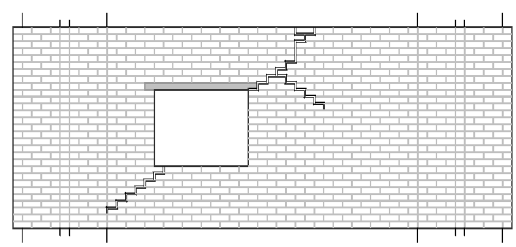

(b) Experimental crack pattern

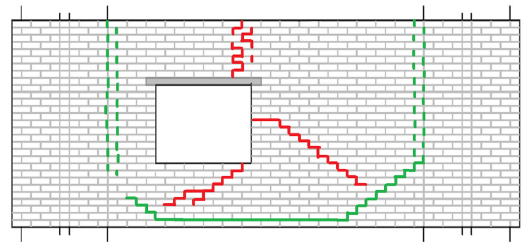

(c) Simulation crack pattern

Material properties: fric=30°; c=0.16 MPa; f_t=0.12 MPa

Horizontal joints

j_{kn}=6.6e3 MPa/m; j_{ks}=5.6e3 MPa/m

Vertical joints

j_{kn}=2.4e3 MPa/m; j_{ks}=2e3 MPa/m

Figure 11: Wall S6

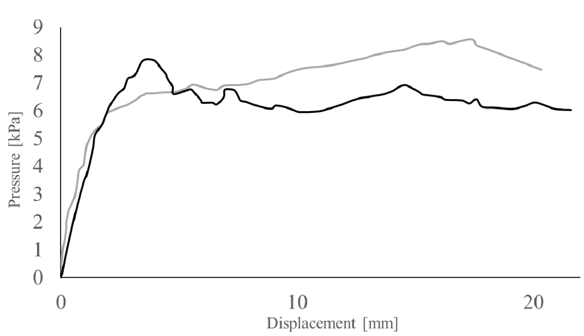

Pressure-displacement diagram

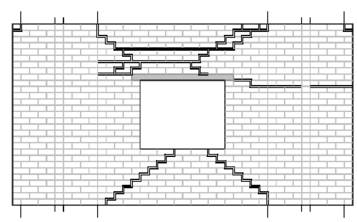

(b) Experimental crack pattern

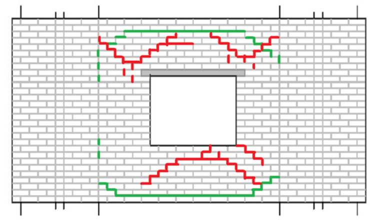

(c) Simulation crack pattern

Material properties: fric=30°; c=0.21 MPa; f_t=0.19 MPa

Horizontal joints

j_{kn}=2.5e3 MPa/m; j_{ks}=2.1e3 MPa/m

Vertical joints

j_{kn}=0.9e3 MPa/m; j_{ks}=0.75e3 MPa/m

Figure 12: Wall S8

4. CONCLUSIONS

Simple brick-mortar tests were modelled to calibrate the material constitutive relations. Simulations of seven walls subjected to out-of-plane loading were performed to gauge the efficiency of DEM and specifically the performance of the 3DEC code to reproduce the non-linear behaviour of masonry.

The performed simulations are a first attempt that can be further refined. The relatively simple model was shown to be capable of reproducing the heterogeneous behaviour of masonry with sufficient accuracy and in reasonable agreement with experimental data. Hence the DEM was demonstrated to be a useful tool to enable a deeper understanding of the behaviour of unreinforced masonry walls when subjected to complex out-of-plane loading conditions.

Horizontal and corner cracks were found to develop at the inner face of the modelled walls. These crack patterns need to be further studied, as a consequence of the boundary conditions and the degree or rotation allowed. Boundary condition degrees of freedom strongly affect the crack pattern and the ultimate strength. Therefore, the next step will be to perform time history analysis with the only boundary condition being the floor.

5. ACKNOWLEDGEMENTS

This research was supported by QuakeCoRE, a New Zealand Tertiary Education Commission-funded Centre.

6. REFERENCES

Baraldi, D., & Cecchi, A. (2017). A full 3D rigid block model for the collapse behaviour of masonry walls. *European Journal of Mechanics - A/Solids, 64*, 11-28. 10.1016/j.euromechsol.2017.01.012

Bui, T. T., & Limam, A. (2013, Sep 2012). *Masonry Walls under Membrane or Bending Loading Cases: Experiments and Discrete Element Analysis*. Paper presented at the The Eleventh International Conference on Computational Structures Technology, Dubrovnik, Croatia

Çaktı, E., Saygılı, Ö., Lemos, J. V., & Oliveira, C. S. (2016). Discrete element modeling of a scaled masonry structure and its validation. *Engineering Structures, 126*, 224-236. 10.1016/j.engstruct.2016.07.044

Giamundo, V., Sarhosis, V., Lignola, G. P., Sheng, Y., & Manfredi, G. (2014). Evaluation of different computational modelling strategies for the analysis of low strength masonry structures. *Engineering Structures, 73*, 160-169. 10.1016/j.engstruct.2014.05.007

Griffith, M. C., & Vaculik, J. (2007). Out-of-Plane Flexural Strength of Unreinforced Clay Brick Masonry Walls. *TMS Journal*

Itasca. (2013). 3DEC (3-Dimensional distinct element code) (Version 4.1.). Minneapolis (MN)

Lawrence, S. J., & Marshal, R. J. (1996). Virtual work appraoch to design of masonry walls under lateral loading *CBPI Technical Manuals*. Clay Brick and paver Institute (CBPI).

Leite, J., Lourenco, P. B., & Ingham, J. M. (2013). Statistical Assessment of Damage to Churches Affected by the 2010–2011 Canterbury (New Zealand) Earthquake Sequence. *Journal of Earthquake Engineering, 17*(1), 73-97. 10.1080/13632469.2012.713562

Lourenço, P. B. (2002). Computations on historic masonry structures. *Progress in Structural Engineering and Materials, 4*(3), 301-319. 10.1002/pse.120

Van der Pluijm, R. (1992). *Material properties of masonry and its components under tension and shear.* Paper presented at the Proc. 6 th Canadian Masonry Symposium, Saskatoon, Saskatchewan, Canada.

Van der Pluijm, R. (1993). *Shear behavior of bed joints.* Paper presented at the Proc. 6 th North American Masonry Conf., Philadelphia, Pennsylvania, USA.

Van der Pluijm, R. (1997). Non-Linear Behaviour of Masonry under tension. *HERON, 42*(1)